Paper:

Characteristics and Individual Differences of Human Actions for Avoiding Harm to Eyes from a Robot

Takamasa Hattori*, Yoji Yamada*, Shogo Okamoto*, Shuji Mori, and Shunsuke Yamada*****

*Graduate School of Engineering, Nagoya University
Furo-cho, Chikusa-ku, Nagoya 464-8603, Japan
E-mail: hattori.takamasa@e.nagoya-u.jp, {yamada-yoji, okamoto-shogo}@mech.nagoya-u.ac.jp
**Faculty of Information Science and Electrical Engineering, Kyushu University
744 Motooka, Nishi-ku, Fukuoka 819-0395, Japan
E-mail: mori@inf.kyushu-u.ac.jp
***Mitsui Chemicals, Inc., Japan
[Received October 21, 2013; accepted May 7, 2014]

To investigate harm-avoidance actions in human beings in close contact with a robot, we conducted psychological experiments in which one of the sharp end effectors of a robot was made to approach the eyes of a facing participant suddenly. We define three parameters for analyzing harm-avoidance actions: avoidance reaction time, maximum avoidance acceleration, and maximum avoidance speed. Results suggest that avoidance reaction time depends on the initial distance between the human eyes and the approaching object, but not on the type of work being performed. We derive a novel nonparametric multiple comparison for statistically testing multivariate data on human actions. Results show that bivariate data for avoidance reaction time and maximum avoidance speed differ for most participants. These findings are expected to contribute positively to determining human-robot conditions for safe coexistence.

Keywords: robot safety, human-robot interaction, harm-avoidance action, psychological experiment

1. Introduction

1.1. Background

The second author of this article previously proposed and developed a next-generation cell production system in which human beings and robots worked cooperatively in practical study [1]. Specifically, light curtains were placed between the human worker and the robot for safety reasons. The safety distance required by light curtains, however, reduces the space available for work. This tends to lower productivity. It would thus be desirable to remove light curtains from production sites.

In doing so, we must consider the basic problem of eye vulnerability compared, for example, to other parts such as the shoulder because the form of a sharp-edged object grasped by a robot cannot be changed to be safer even when the robot is designed to be inherently safe. Eye safety must therefore be considered to ensure a safe working environment.

Human beings naturally exhibit harm-avoidance behavior when a threat is perceived, so the possibility of avoiding or limiting harm (hereafter "avoidability"), described as one risk element in international standard [2], must be considered in determining safe human-robot conditions. Avoidability currently tends to be either neglected or estimated intuitively, however, because harm avoidance is a relatively unexplored human factor. The characteristics of harm-avoidance actions must be investigated to determine human-robot conditions that allow for safe coexistence.

Here, a robot entering a runaway state cannot be stopped immediately because it keeps moving during the time interval from the detection of the runaway state by self-diagnosis functions to the time at which the robot is completely stopped by brakes. If a human being cannot escape from the space through which the robot can move during this time interval, the human being and the robot may collide. It is therefore important to investigate human harm-avoidance actions against robot motion under the premise that a robot enters a runaway state in order to consider human-robot conditions for safe coexistence.

1.2. Related Studies

Previous research on the safety of human-robot interaction focused mainly on the end results of harmful interaction. Yamada [3], for example, investigated human pain tolerance by conducting experiments in which mechanical stimuli were applied to a participant. Oberer and Schraft [4] investigated injury indices by simulating collisions of a robot with the head, chest, and pelvis of a dummy by using finite element models, and Haddadin et al. [5] followed up with head and chest collision experiments. Our group investigated injury severity by conducting experiments in which the sharp end effector of a robot collided with a dummy eye [6].

Human reactions to robot approaches have been investigated in some studies. In [7], researchers measured the time for starting an escape action and the trajectory of the

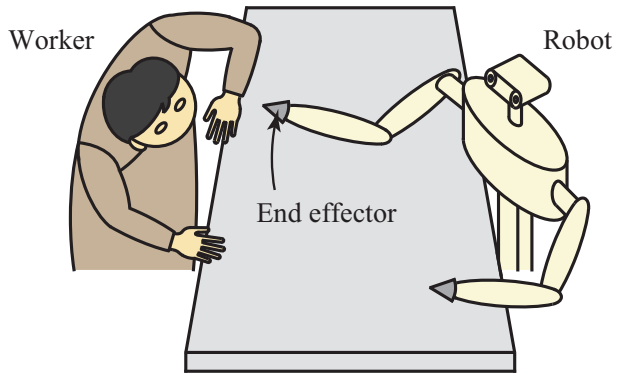

Fig. 1. The assumed situation.

action for a participant who focused on a robot manipulator and was suddenly confronted by an erroneous manipulator motion. To investigate which robot motions were regarded as threatening, Ikeura et al. [8] measured the galvanic skin reflex when a robot moved straight toward a participant's face. To identify robot motion conditions that triggered human fear, Yamada et al. [9] measured the pupil diameter when a robot end effector was accelerated toward a participant's face.

Statistical investigations on harm-avoidance actions have yet to be conducted, however.

1.3. Study Objectives

We designed psychological experiments to investigate human harm-avoidance actions during a situation in which the eyes of a human being sitting in front of a robot were threatened during human-robot interaction based on the runaway assumption [10].[1] We investigated whether harm-avoidance actions are influenced by the type of work being performed or by the initial distance between the human eyes and the robot end effector [11, 12]. We then investigated individual differences in human reaction time (RT) and human motion performance triggered by the sudden approach of the end effector [12]. While analyzing human factors, we here derive a novel multiple comparison for statistically testing multivariate data on human actions for which parametric tests are not applicable. This article details our novel analyses, which contribute to reasonable estimations of avoidability.

2. Psychological Experiment I

We consider a situation in which a robot gripper or the grasped object becomes a mechanical hazard. In reference to practical study [1], we assume a situation in which one of the sharp end effectors of a production-site robot suddenly approaches the eyes of a worker sitting opposite, as shown in **Fig. 1**.

1. This study was approved by the Nagoya University ethics committee.

Fig. 2. Upper-body humanoid.

The worker can, in principle, initiate harm-avoidance behavior based on both visual and auditory information. Workers may not necessarily hear robot's motors, however, in an actual working environment, so we focused on a more hazardous situation in which only visual information is available to the worker.

2.1. Experiment Overview

Four types of tasks were set that simulated work performed at production sites. The objective of this experiment was to investigate whether harm-avoidance actions are influenced by the type of task.

2.1.1. Apparatus

An upper-body humanoid robot (HIRO, Kawada Industries, Inc.), designed to operate collaboratively with human beings [1, 13], was used. A photograph of the robot is shown in **Fig. 2**. This robot is controlled by being set to output the highest possible speed percentage, and the speed pattern cannot be changed at will. The participant, who wore protective glasses, faced the robot across a work table. To minimize risk to the participant, end effectors originally used for picking up and placing mechanical parts were replaced by pyramids made of flexible polyurethane foam.

2.1.2. Participants

We recruited students who were unfamiliar with robotics to take part. The 11 participants in this experiment were six males and five females aged 19 to 28. All

(a) Tasks A and D (b) Task B

Fig. 3. Bearing rings used in tasks.

were healthy with good eyesight,[2] with none reported to have belonephobia.[3]

2.1.3. Experiment Setup

Each participant wore a cap having motion capture markers and sat on a stool in front of the robot. We instructed participants to maintain postures in which they could perform tasks easily. Participants wore noise-canceling earphones (NW-A845, Sony Corporation) to prevent the entry of external auditory information, listening instead to sounds recorded in a factory. Participants were exposed to the robot's work area and performed the following four tasks.

Task A: Using tweezers to insert two mechanical parts, rollers and retainers, between bearing rings.

Task B: Using tweezers to remove rollers from between bearing rings.

Task C: Silently reading a document on a liquid crystal display (LCD).

Task D: Gazing at parts between bearing rings.

Tasks A, B, and D were conducted with the bearing rings shown in **Fig. 3**. Task A was performed similarly to the way workers perform the task in actual production.

While the participant concentrated on these tasks, the robot initially was idle, and then the robot suddenly moved one end effector on its arm toward the eyes of the participant.[4] We instructed the participant to react naturally. The movements of the participant and robot were captured by a video camera, with a motion capture system (Motion Analysis Corporation) recording the participant's head movement at a sampling rate of 60 Hz.

2.2. Experiment Conditions

The probability distribution of the foreperiod[5] for a participant not aware of presentation timing of a stimulus is often modeled using exponential distribution [14], so statistically random foreperiods were determined by taking the sum of 10 s and an exponentially distributed random value of mean 20 s. Foreperiods longer than 90 s were excluded.

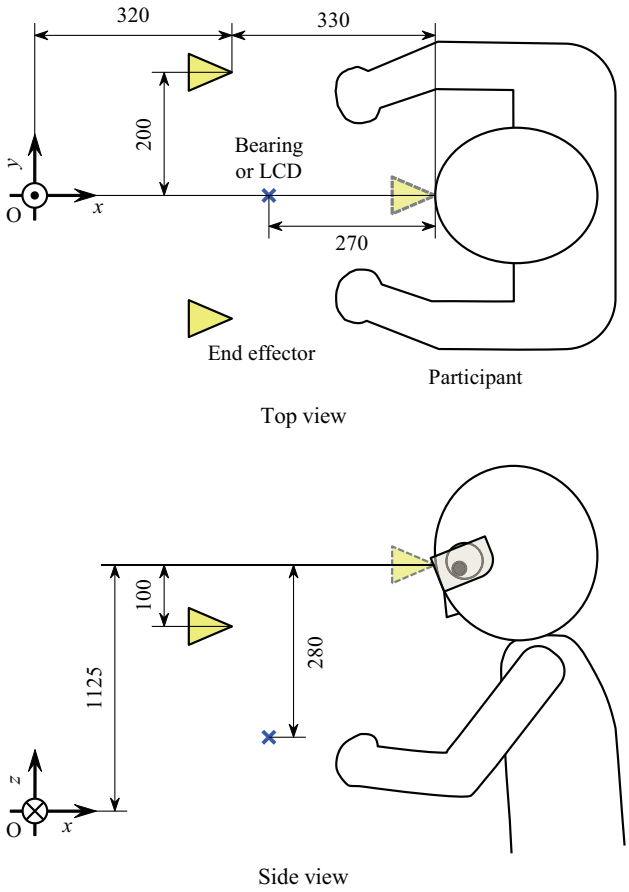

Fig. 4. Interactive human-robot locations in psychological experiment I (unit: mm).

Figure 4 shows locations and distances in this experiment. The device for the task – bearing rings or the LCD – was located at the position indicated by the bold "×." The initial distance between the participant's eyes and the end effector was approximately 400 mm.[6] Each participant was asked to confirm that the end-effector tips were within peripheral view when located at a viewing angle of approximately 40° with the task position in the center of the visual field. In a trial, the end-effector tip arrived near the participant's initial eye position at the end of robot motion.

Figure 5 shows the speed pattern of the end-effector tip assuming that the robot had entered a runaway state. The approach paths of both end effectors were elliptical and symmetrical, and the approach motion pattern was the same in each trial.

2. For safety reasons, initial experiments had to be conducted with young people in good health who appeared to have good reactions.
3. "Belonephobia" means fear of sharply pointed objects.
4. Participants were told in advance that the end effector would approach their eyes.
5. "Foreperiod" means the time interval from the beginning of a trial to the beginning of stimulus presentation.
6. When robots are introduced to a mobile phone cell production site, for example, the initial distance is assumed to be hundreds of millimeters.

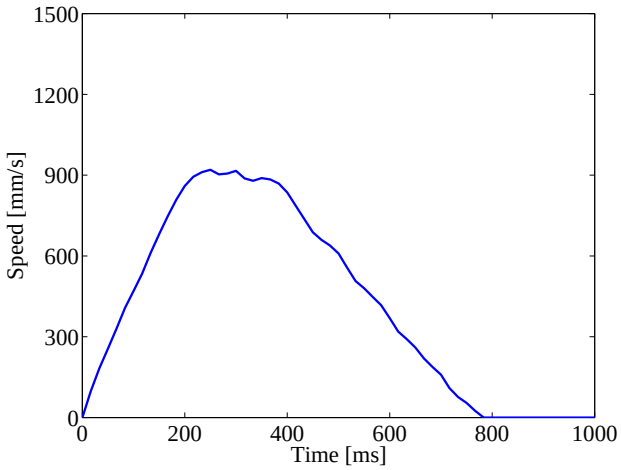

Fig. 5. Speed pattern of the robot's end-effector tip in psychological experiment I.

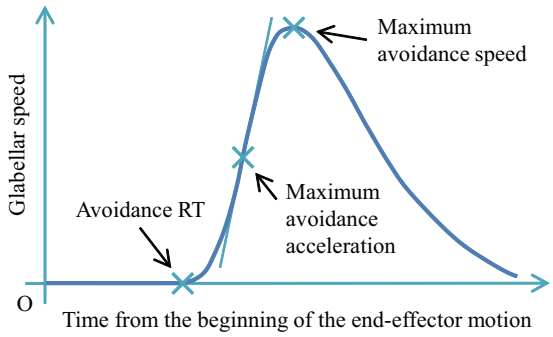

Fig. 6. Definition of avoidance action parameters.

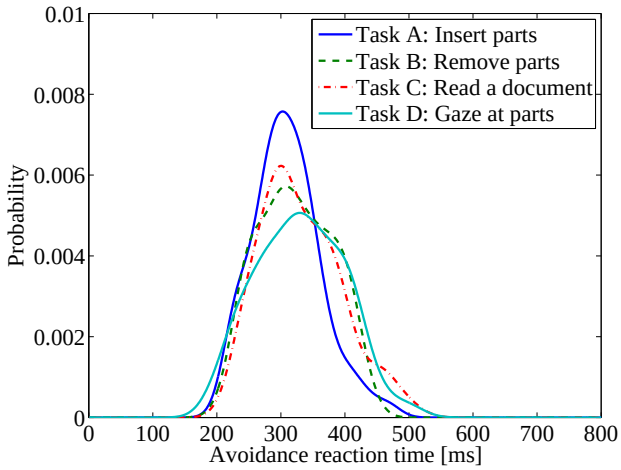

Fig. 7. Probability distribution of avoidance RT for all types of tasks.

Table 1. Steel-Dwass tests for differences in avoidance RT between tasks.

Tasks	Two-sided p-value
A & B	$p > 0.20$
A & C	$0.10 < p < 0.20$
A & D	$p > 0.20$
B & C	$p > 0.20$
B & D	$p > 0.20$
C & D	$p > 0.20$

2.3. Experiment Procedure

Each participant performed 24 trials, i.e., six trials for each of the four tasks. Tasks were assigned in random order to prevent any effects due to their order. The approaching end effector was also chosen at random for each trial.

2.4. Experiment Results

2.4.1. Probability Distribution of Avoidance RT

Avoidance reaction time (RT) is defined as the time interval from the beginning of end-effector motion to the beginning of the participant's head movement[7] as shown in **Fig. 6**.

Figure 7 shows the probability distribution of avoidance RT estimated for each task based on data from all participants as calculated by the method presented in Appendix A. This figure shows that the positions of leading edges and distribution peaks do not differ notably.

2.4.2. Statistical Analysis of Avoidance RT

Statistical tests were carried out to investigate whether the task had any effect on avoidance RT. Because the population could not be assumed to be normal, we used the Steel-Dwass test [15, 16], which is a nonparametric test for investigating, with control of the type I error, whether the difference between two of more than three groups is significant. The null hypothesis was that avoidance RTs for each pair of tasks were identical. **Table 1** summarizes Steel-Dwass test results based on avoidance RT data from all participants, showing that no difference is significant at the $\alpha = 0.05$ significance level, so avoidance RT does not appear to depend on the type of task.

2.4.3. Statistical Analysis of the Effect of Participant Posture in Avoidance RT

We consider the possibility that a participant's posture at the moment the end effector began to move affected avoidance RT, denoting the x-coordinate of the participant's eyes at this moment as x_{e1} and regarding the position of the eyes to be that of the glabella.[8] The median of x_{e1} for all participants is denoted by $\tilde{x}_{e1}$, and all trials were divided into type F – those in which $x_{e1} < \tilde{x}_{e1}$ – and type B – those in which $x_{e1} > \tilde{x}_{e1}$. That is, type F trials are those in which the participant slouched while seated.

For this test, we used the Mann-Whitney U-test [17], which is a nonparametric test for the difference between two groups. The null hypothesis was that avoidance

7. No participants protected their faces with their arms.

8. "Glabella" means the smooth area between the eyebrows just above the nose.

RTs for trials F and B were identical. The difference in avoidance RT between trials F and B was significant at the $\alpha = 0.001$ level (difference = 33 ms, two-sided, $p = 1.98 \times 10^{-4}$). This result suggests that avoidance RT is shorter when the participant is slouching.

3. Psychological Experiment II

3.1. Experiment Overview

When the participant sits slouching, the initial distance between the participant's eyes and the robot end effector is shorter, so results of psychological experiment I suggest that harm-avoidance actions are contingent on the initial distance between the human eyes and the end effector. To clarify this dependence, psychological experiment II was conducted with three different initial positions for end effectors. The experimental setup and conditions are similar to those in psychological experiment I except as indicated below.

3.1.1. Participants

The nine participants in this experiment were five males and four females aged 18 to 28. Some had also participated in psychological experiment I.

3.1.2. Experiment Setup

Each participant was exposed to the robot's work area and performed task A of psychological experiment I.

3.2. Experiment Conditions

Statistically random foreperiods were determined by taking the sum of 10 s and an exponentially distributed random value of mean 15 s. Foreperiods longer than 60 s were excluded.

Figure 8 shows locations and distances in this experiment. Bearing rings were located at the position indicated by the bold "×." Three patterns were chosen for the initial positions of end effectors. The initial distance between the participant's eyes and the end effector was approximately 470 mm for pattern 1, 370 mm for pattern 2, and 270 mm for pattern 3. Each participant was asked to confirm that the end-effector tips were within peripheral view when located at a viewing angle of approximately 30° for all patterns with the task position in the center of the visual field. In a trial, the end-effector tip arrived at a point approximately 50 mm forward in relation to the participant's initial eye position at the end of robot motion.

Figure 9 shows the speed pattern of the end-effector tip based on the runaway assumption.[9]

3.3. experiment Procedure

Each participant performed 60 trials, with the end-effector pattern and approaching end effector both chosen at random for each trial.

9. We set the robot to output the same highest possible speed percentage for each pattern. While the initial acceleration was similar to each other, the maximum speed inevitably decreased as the travel distance decreased.

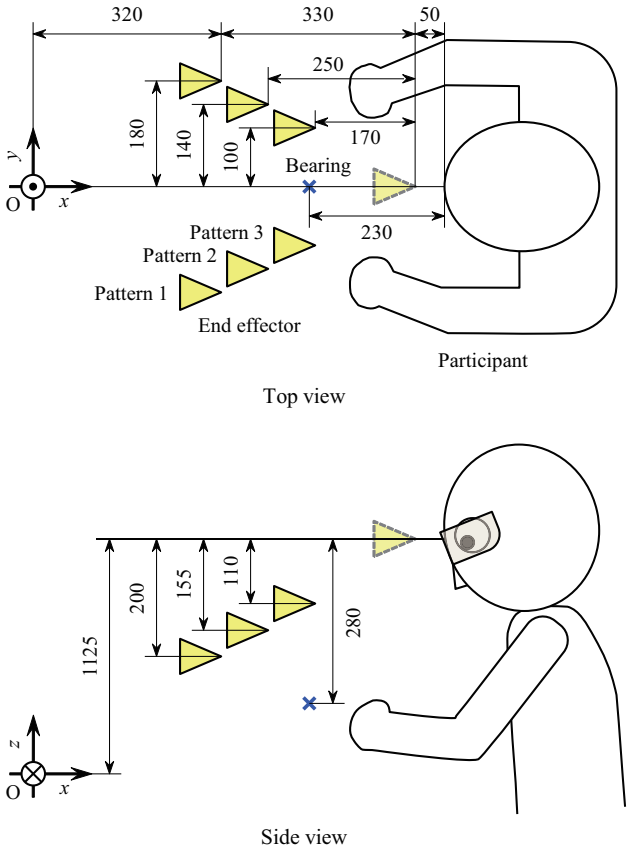

Fig. 8. Interactive human-robot locations in psychological experiment II (unit: mm).

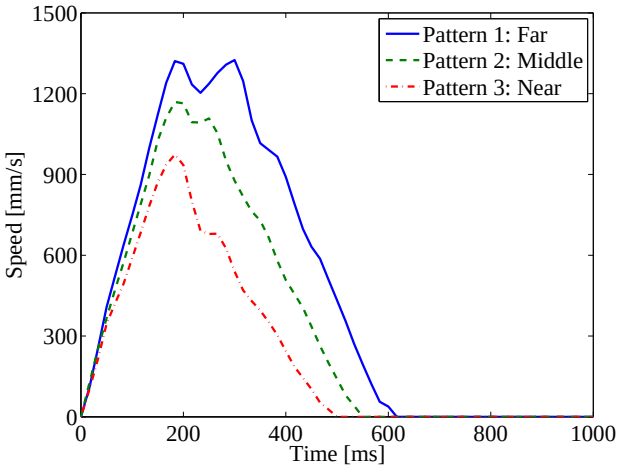

Fig. 9. Speed pattern of the robot's end-effector tip in psychological experiment II.

3.4. Experiment Results

3.4.1. Probability Distribution of Avoidance RT

Figure 10 shows the probability distribution of avoidance RT estimated for each end-effector pattern based on data from all participants as calculated by the method presented in Appendix A. This figure shows that the peak position is different for each distribution. There is a ten-

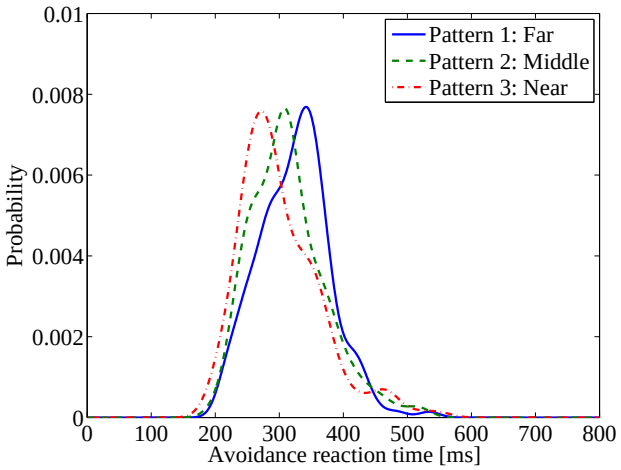

Fig. 10. Probability distribution of avoidance RT for all types of patterns.

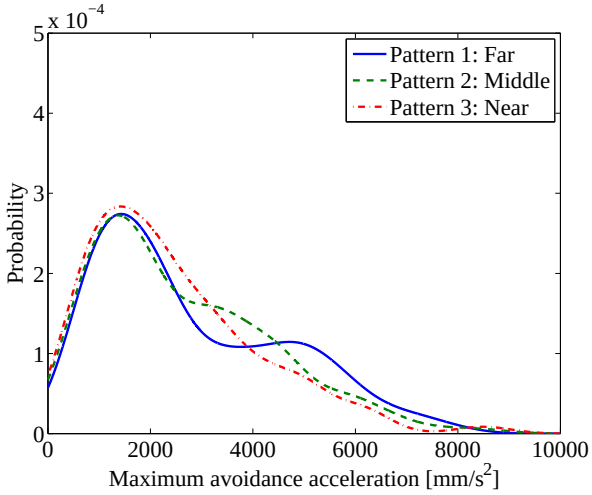

Fig. 11. Probability distribution of maximum avoidance acceleration for all types of patterns.

Table 2. Steel-Dwass tests for differences in avoidance RT between patterns.

Patterns	Two-sided p-value
1 & 2	$0.05 < p < 0.10$
1 & 3	$p < 0.0001$
2 & 3	$0.025 < p < 0.05$

Table 3. Steel-Dwass tests for differences in maximum avoidance acceleration between patterns.

Patterns	Two-sided p-value
1 & 2	$p > 0.20$
1 & 3	$p > 0.20$
2 & 3	$p > 0.20$

dency for a shorter initial distance between the human eyes and the end effector to result in shorter avoidance RT.

3.4.2. Statistical Analysis of Avoidance RT

Steel-Dwass tests were carried out to investigate whether the end-effector pattern had any effect on avoidance RT. The null hypothesis was that avoidance RTs for each pair of patterns were identical. **Table 2** summarizes Steel-Dwass test results based on avoidance RT data from all participants. These results suggest that a shorter initial distance between the human eyes and the end effector is associated with shorter avoidance RT.

3.4.3. Probability Distribution of Maximum Avoidance Acceleration

Maximum avoidance acceleration is defined as the maximum acceleration of movement at the participant's glabella as shown in **Fig. 6**.

Figure 11 shows the probability distribution of maximum avoidance acceleration estimated for each end-effector pattern based on data from all participants as calculated by the method presented in Appendix A. This figure shows that the positions of first distribution peaks do not differ notably.[10]

3.4.4. Statistical Analysis of Maximum Avoidance Acceleration

Steel-Dwass tests were carried out to investigate whether the end-effector pattern had any effect on maximum avoidance acceleration. The null hypothesis was that maximum avoidance acceleration for each pair of patterns was identical. **Table 3** summarizes Steel-Dwass test results based on maximum avoidance acceleration data from all participants. No significant difference was found at a significance level of $\alpha = 0.05$, so maximum avoidance acceleration does not appear to depend on the initial distance between the human eyes and the end effector.

3.4.5. Probability Distribution of Maximum Avoidance Speed

Maximum avoidance speed is defined as the maximum speed of movement at the participant's glabella as shown in **Fig. 6**.

Figure 12 shows the probability distribution of maximum avoidance speed estimated for each end-effector pattern based on data from all participants as calculated by the method presented in Appendix A. This figure shows that the positions of first distribution peaks do not differ notably.[11]

10. The probability distribution in pattern 1 has a second peak resulting mainly from data on participants A, F, and H.

11. The probability distribution in patterns 1 and 3 has a second peak resulting mainly from data on participants A, F, and H.

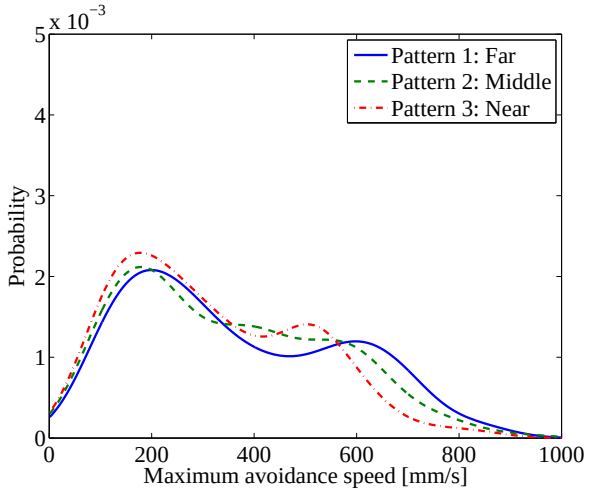

Fig. 12. Probability distribution of maximum avoidance speed for all types of patterns.

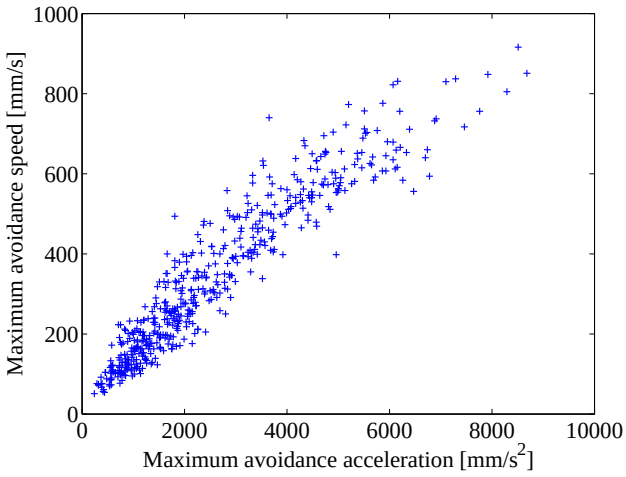

Fig. 13. Relationship between maximum avoidance acceleration and maximum avoidance speed.

Table 4. Steel-Dwass tests for differences in maximum avoidance speed between patterns.

Patterns	Two-sided p-value
1 & 2	$p > 0.20$
1 & 3	$0.10 < p < 0.20$
2 & 3	$p > 0.20$

3.4.6. Statistical Analysis of Maximum Avoidance Speed

Steel-Dwass tests were carried out to investigate whether the end-effector pattern had any effect on maximum avoidance speed. The null hypothesis was that maximum avoidance speed for each pair of patterns was identical. No significant difference was found (**Table 4**), so maximum avoidance speed does not appear to depend on the initial distance between the human eyes and the end effector.

3.4.7. Relationships between Avoidance Action Parameters

We focused on the relationships between avoidance action parameters, i.e., avoidance RT, maximum avoidance acceleration, and maximum avoidance speed.

Figure 13 shows the relationship between maximum avoidance acceleration and maximum avoidance speed based on data from all participants. There seems a strong positive correlation between the two parameters. This correlation was significant at the $\alpha = 0.001$ level (Spearman rank correlation coefficient [18, 19] $r_S = 0.950$, two-sided, $p = 2.66 \times 10^{-265}$). The value of acceleration cannot, in general, be determined more easily in analyses than that of speed. On this basis, we concluded that maximum avoidance acceleration is not always necessary for analyses, and therefore deal only with avoidance RT and maximum avoidance speed in the following analyses.

When carrying out extrapolation simulation of human-robot collision [20][12] focusing on a participant who has a lower ability to avoid harm, simulation results provide motion conditions of the end effector that ensure safety for all participants, so we investigated individual differences in avoidance action parameters. **Figs. 14**, **15**, and **16** show the relationships between avoidance RT and maximum avoidance speed based on data from each participant in patterns 1, 2, and 3. In these figures, there seem to be large differences in avoidance action parameters between participants, even though trends in the figures are similar to each other. In results of extrapolation simulation [20], the human-robot location in pattern 3 seems most hazardous, so we deal with only pattern 3 in the following analysis.

3.4.8. Multivariate Statistical Analysis of Individual Differences in Avoidance Action Parameters

When investigating individual differences in avoidance action parameters using the Steel-Dwass test, the number of pairs to be compared during statistical analyses increases directly with the number of avoidance action parameters. Here we consider treating avoidance action parameters as multivariate data and investigating individual differences in multivariate data. The Steel-Dwass test cannot be used for this investigation because this test is for univariate data, so we extended the Steel-Dwass test to a multivariate test (Appendix B).

Multivariate Steel-Dwass tests were carried out to investigate whether bivariate data for avoidance RT and maximum avoidance speed in pattern 3 differed between participants. The null hypothesis was that bivariate data for each pair of participants in pattern 3 were identical. **Table 5** summarizes results. Labels A–I denote participants. A single asterisk ($*$) denotes differences that are significant at significance level $\alpha = 0.05$ and double asterisks ($**$) those significant at $\alpha = 0.01$. An entry of n.s.

12. Extrapolation simulation simulates collision situations in which psychological experiments cannot be designed for safety reasons.

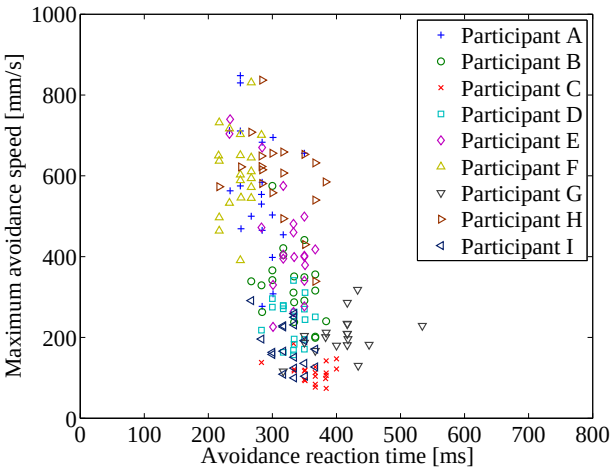

Fig. 14. Relationship between avoidance RT and maximum avoidance speed among participants in pattern 1.

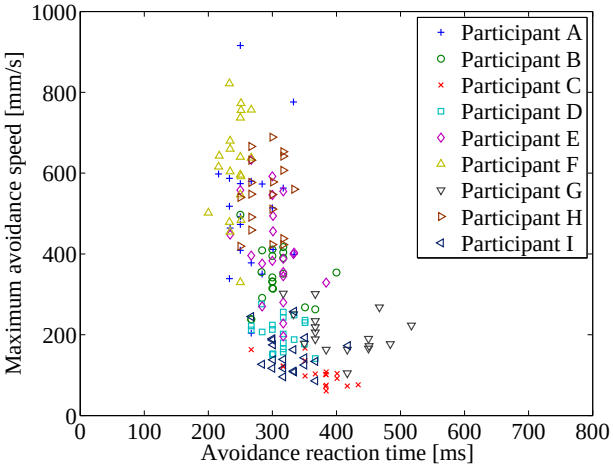

Fig. 15. Relationship between avoidance RT and maximum avoidance speed among participants in pattern 2.

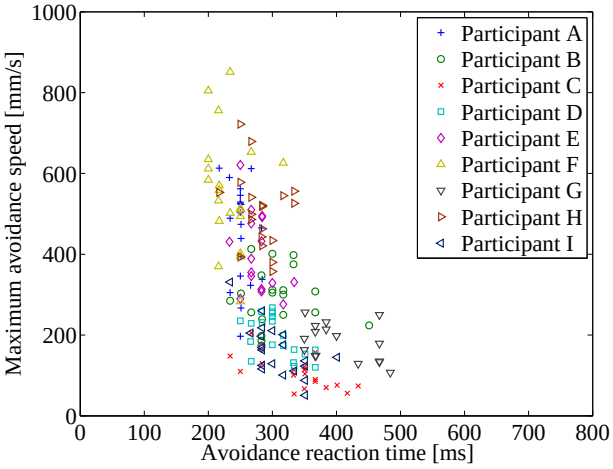

Fig. 16. Relationship between avoidance RT and maximum avoidance speed among participants in pattern 3.

Table 5. Multivariate Steel-Dwass tests for differences in avoidance RT and maximum avoidance speed among participants in pattern 3.

	B	C	D	E	F	G	H	I
A	**	**	**	n.s.	n.s.	**	*	**
B		**	*	n.s.	**	**	**	**
C			**	**	**	**	**	n.s.
D				**	**	**	**	n.s.
E					**	**	n.s.	**
F						**	**	**
G							**	**
H								**

means that the difference is not significant at $\alpha = 0.05$. The table shows that bivariate data for avoidance RT and maximum avoidance speed in pattern 3 differ for most pairs of participants.

4. Discussion

Even though types of tasks and end-effector patterns were limited, we could determine harm-avoidance action characteristics under experimental conditions.

4.1. Influence of Approach Velocity

The velocity of an approaching object is likely to be an important factor in determining harm-avoidance action characteristics. Differences in the maximum speed of the robot's end-effector tip may have affected avoidance RT in psychological experiment II. The initial and maximum speeds for pattern 3 in psychological experiment II are similar to those in psychological experiment I, but avoidance RT for pattern 3 in psychological experiment II was shorter. We thus concluded that avoidance RT was, instead, mainly influenced by the initial distance between the participant's eyes and the end effector.

4.2. Influence of Cognitive Processes

It seems possible to consider that participants may have expected the approaching end effector in experiments. This is based on the idea that harm-avoidance actions are associated with human cognitive processes. In contrast, we consider harm-avoidance actions to be reflexive processes with reference to results of psychological experiment I showing that avoidance RT does not appear to depend on the type of work. This consideration can be associated with experimental results in [21] showing that monkeys withdrew abruptly in response to the stimulus of looming,[13] and no evidence of habituation or extinction

13. "Looming" means the optical stimulus consisting of the expansion of a closed contour in the visual field [21, 22].

was found. We cannot, however, rule out cognitive influences at this point. Nevertheless, avoidance RT distribution that statistically represents harm-avoidance action characteristics can be used to reasonably estimate avoidability. For a simple example, based on the fact that the longest avoidance RT is approximately 550 ms as shown in **Figs. 7** and **10**, we can evaluate whether sufficient distance is provided in the treated situation for preventing human-robot collision.

4.3. Individual Differences in Harm-Avoidance Actions

Using a novel nonparametric test we devised for multiple comparisons (Appendix B), we could easily investigate individual differences in avoidance action parameters in psychological experiment II because the number of pairs compared decreased from 72 to 36. From the viewpoint of estimating avoidability, we should focus on a participant with parameter values in lower right areas of **Figs. 14**, **15**, and **16** because the participant has a lower ability to avoid harm. This is similar to the approach used for investigating people with higher athletic ability in sports science.

4.4. Human-Robot Conditions for Safe Coexistence

We investigated characteristics and individual differences of harm-avoidance actions under the premise that a robot entered a runaway state. Assuming that each joint of the robot enters the runaway state based on uniform probability distribution, the maximum space through which the robot can move during the runaway can be calculated using the concept of manipulability ellipsoid. Hence, when quantitative extrapolation simulation [20] extended by introducing the concept of manipulability ellipsoid is carried out focusing on a person who has a lower ability to avoid harm, we can discuss whether the person can escape from the space. We can then consider escapable conditions of the person as human-robot conditions for safe coexistence.

5. Conclusions

We have conducted psychological experiments to investigate human harm-avoidance actions under a scenario in which the sharp end effector of a robot suddenly approaches the eyes of a human being sitting in front of the robot, assuming further that the robot has entered a runaway state. Results of psychological experiment I did not suggest that avoidance reaction time (RT) depended on the type of work, but did suggest that participant posture, i.e., slouching, affected avoidance RT. Results of psychological experiment II have suggested that avoidance RT depends on the initial distance between the human eyes and the approaching object, but that neither maximum avoidance acceleration nor maximum avoidance speed did. We have developed a novel nonparametric multiple comparison for statistically testing multivariate data. Using this test, we have found that bivariate data for avoidance RT and maximum avoidance speed differ for most pairs of participants in psychological experiment II.

Although there remains the issue of whether the three parameters, i.e., avoidance RT, maximum avoidance acceleration, and maximum avoidance speed, are most important for estimating avoidability, these findings are expected to contribute to managing human-robot coexistence space by taking avoidability into consideration.

The results of this study are general in terms of dealing with a common problem in human-robot interaction in which a sharp-edged object grasped by a robot may cause serious injury to the human eye. The situation studied, where a human being sat in front of a robot, applies not only to other production-site robots but also to other cases, such as a home robot grasping a pen.

Acknowledgements

We are indebted to Professor Kazuo Koga of Kyoto Notre Dame University for his insightful advice. We also thank former graduate students Soichiro Ito and Koji Sunada of Nagoya University for their cooperation. This work was supported in part by MEXT KAKENHI Grant Number 21246041.

References:

[1] New Energy and Industrial Technology Development Organization, "Project for Strategic Development of Advanced Robotics Elemental Technologies, Human-Robot Cooperative Cell Production and Assembly Systems (Field of Next-Generation Industrial Robots), Safe Upper-Body Humanoid Equipped with Compact Handling Systems," Accomplishment report in fiscal 2006-2008, May 2009 (in Japanese).

[2] "Safety of Machinery – General Principles for Design – Risk Assessment and Risk Reduction," ISO 12100:2010, 2010.

[3] Y. Yamada, "Evaluation of Human Pain Tolerance and Its Application to Designing Safety Robot Mechanisms for Human-Robot Coexistence," J. of Robotics and Mechatronics, Vol.9, No.1, pp. 65-70, 1997.

[4] S. Oberer and R. D. Schraft, "Robot-Dummy Crash Tests for Robot Safety Assessment," In Proc. of the 2007 IEEE Int. Conf. on Robotics and Automation, pp. 2934-2939, Roma, Italy, Apr. 2007.

[5] S. Haddadin, A. Albu-Schäffer, M. Frommberger, J. Rossmann, and G. Hirzinger, "The "DLR Crash Report": Towards a Standard Crash-Testing Protocol for Robot Safety – Part I: Results," In Proc. of the 2009 IEEE Int. Conf. on Robotics and Automation, pp. 272-279, Kobe, Japan, May 2009.

[6] S. Ito, Y. Yamada, T. Hattori, S. Okamoto, and S. Hara, "Basic Experiments on Collision of Sharp Mechanical Hazards against Eye for Estimation of Injury Severity," In Proc. of the 2012 IEEE Int. Conf. on Robotics and Biomimetics, pp. 1912-1917, Guangzhou, China, Dec. 2012.

[7] Japan Industrial Robot Association, "Study on Standardization of Industrial Robots in Fiscal 1987," Mar. 1988 (in Japanese).

[8] R. Ikeura, H. Otsuka, and H. Inooka, "Study on Emotional Evaluation of Robot Motions Based on Galvanic Skin Reflex," The Japanese J. of Ergonomics, Vol.31, No.5, pp. 355-358, Oct. 1995 (in Japanese).

[9] Y. Yamada, Y. Umetani, and Y. Hirasawa, "Proposal of a Psychophysiological Experiment System Applying the Reaction of Human Pupillary Dilation to Frightening Robot Motions," In Proc. of the 1999 IEEE Int. Conf. on Systems, Man, and Cybernetics, Vol.2, pp. 1052-1057, Tokyo, Japan, Oct. 1999.

[10] T. Hattori, Y. Yamada, S. Mori, S. Esaki, and S. Hara, "A Study on Harm-Avoidance Behavioral Characteristics Based on Psychological Experiments for Human-Robot Coexistence Systems," IEICE Technical Report, Vol.110, No.98, pp. 7-10, Jun. 2010 (in Japanese).

[11] T. Hattori, Y. Yamada, S. Mori, S. Okamoto, and S. Hara, "Psychological Experiments on Avoidance Action Characteristics for Estimating Avoidability of Harm to Eyes from Robots," In Proc. of

the 2012 IEEE/RSJ Int. Conf. on Intelligent Robots and Systems, pp. 5400-5405, Vilamoura, Portugal, Oct. 2012.
[12] T. Hattori, Y. Yamada, S. Okamoto, S. Mori, S. Yamada, and S. Hara, "Study on Avoidance Action Parameters against a Sharp End-Effector Tip Approaching Human's Eyes," In Proc. of the 21st IEEE Int. Symposium on Robot and Human Interactive Communication, pp. 25-30, Paris, France, Sep. 2012.
[13] T. Ogure, Y. Nakabo, S. Jeong, and Y. Yamada, "Hazard Analysis of an Industrial Upper-Body Humanoid," Industrial Robot: An Int. J., Vol.36, No.5, pp. 469-476, Aug. 2009.
[14] R. D. Luce, "Response Times: Their Role in Inferring Elementary Mental Organization," Oxford University Press, New York, NY, 1986.
[15] R. G. D. Steel, "A Rank Sum Test for Comparing All Pairs of Treatments," Technometrics, Vol.2, No.2, pp. 197-207, May 1960.
[16] M. Dwass, "Some *k*-Sample Rank-Order Tests," In I. Olkin, S. G. Ghurye, W. Hoeffding, W. G. Madow, and H. B. Mann (Eds.), Contributions to Probability and Statistics: Essays in Honor of Harold Hotelling, chapter 17, pp. 198-202, Stanford University Press, Stanford, CA, 1960.
[17] H. B. Mann and D. R. Whitney, "On a Test of Whether One of Two Random Variables Is Stochastically Larger Than the Other," The Annals of Mathematical Statistics, Vol.18, No.1, pp. 50-60, Mar. 1947.
[18] C. Spearman, "The Proof and Measurement of Association between Two Things," The American J. of Psychology, Vol.15, No.1, pp. 72-101, Jan. 1904.
[19] C. Spearman, "'Footrule' for Measuring Correlation," British J. of Psychology, Vol.2, No.1, pp. 89-108, Jul. 1906.
[20] K. Sunada, Y. Yamada, T. Hattori, S. Okamoto, and S. Hara, "Extrapolation Simulation for Estimating Human Avoidability in Human-Robot Coexistence Systems," In Proc. of the 21st IEEE Int. Symposium on Robot and Human Interactive Communication, pp. 785-790, Paris, France, Sep. 2012.
[21] W. Schiff, J. A. Caviness, and J. J. Gibson, "Persistent Fear Responses in Rhesus Monkeys to the Optical Stimulus of "Looming"," Science, Vol.136, No.3520, pp. 982-983, Jun. 1962.
[22] J. J. Gibson, "Visually Controlled Locomotion and Visual Orientation in Animals," British J. of Psychology, Vol.49, No.3, pp. 182-194, Aug. 1958.
[23] E. Parzen, "On Estimation of a Probability Density Function and Mode," The Annals of Mathematical Statistics, Vol.33, No.3, pp. 1065-1076, Sep. 1962.
[24] B. W. Silverman, "Density Estimation for Statistics and Data Analysis," Chapman and Hall, London, UK, 1986.
[25] H. Oja and R. H. Randles, "Multivariate Nonparametric Tests," Statistical Science, Vol.19, No.4, pp. 598-605, Nov. 2004.
[26] T. Royen, "Tables for Studentized Multivariate Maximum Ranges and Their Application by Maximum Range Tests," Biometrical J., Vol.32, No.6, pp. 643-680, 1990.

Appendix A. Method for Estimating Probability Distribution

We estimated probability distribution from data using the kernel estimator [23], which has the advantage of providing smooth distribution. The probability density function of variable x is estimated as

$$\hat{f}(x) = \frac{1}{nh}\sum_{i=1}^{n} k\left(\frac{x-x_i}{h}\right), \quad \ldots\ldots\ldots \quad (1)$$

where n is the number of observations, x_i is the i-th observation, h is the bandwidth, and $k(x)$ is the kernel function. Here, the standard normal probability density function is used for $k(x)$:

$$k(x) = \frac{1}{\sqrt{2\pi}}\exp\left(-\frac{x^2}{2}\right). \quad \ldots\ldots\ldots \quad (2)$$

The bandwidth is calculated by the method proposed by Silverman [24]:

$$h = \frac{0.9}{n^{\frac{1}{5}}}\min\left(s, \frac{q_3-q_1}{1.34}\right), \quad \ldots\ldots\ldots \quad (3)$$

where s, q_1, and q_3 are the standard deviation and the first and third quartiles of data. Accordingly, $q_3 - q_1$ is the interquartile range of data.

Appendix B. Multivariate Steel-Dwass Test Procedure

We extended the Steel-Dwass test to a multivariate test using the affine-invariant spatial rank [25]. When i-th and j-th of c groups of d-variate data are considered, the affine-invariant spatial rank of $\boldsymbol{x}_{ik} \in \mathbf{R}^{d\times 1}$, which is the k-th observation from the i-th group, is given by

$$\boldsymbol{r}_{ik}^{(j)} = \frac{1}{n_i+n_j}\left\{\sum_{l=1}^{n_i}\boldsymbol{u}\left(\boldsymbol{S}^{-\frac{1}{2}}(\boldsymbol{x}_{ik}-\boldsymbol{x}_{il})\right) + \sum_{l=1}^{n_j}\boldsymbol{u}\left(\boldsymbol{S}^{-\frac{1}{2}}(\boldsymbol{x}_{ik}-\boldsymbol{x}_{jl})\right)\right\} \in \mathbf{R}^{d\times 1}, \quad (4)$$

where n_i is the number of observations in the i-th group, $\boldsymbol{S}^{-1/2} \in \mathbf{R}^{d\times d}$ is the transformation matrix, and $\boldsymbol{u}(\boldsymbol{x})$ is the spatial sign function

$$\boldsymbol{u}(\boldsymbol{x}) = \begin{cases} |\boldsymbol{x}|^{-1}\boldsymbol{x} & \text{if } \boldsymbol{x} \neq \mathbf{0}, \\ \mathbf{0} & \text{if } \boldsymbol{x} = \mathbf{0}. \end{cases} \quad \ldots\ldots\ldots \quad (5)$$

Transformation matrix $\boldsymbol{S}^{-1/2}$ is determined to satisfy

$$d\left(\sum_{k=1}^{n_i}\boldsymbol{r}_{ik}^{(j)}\boldsymbol{r}_{ik}^{(j)\mathrm{T}} + \sum_{k=1}^{n_j}\boldsymbol{r}_{jk}^{(i)}\boldsymbol{r}_{jk}^{(i)\mathrm{T}}\right) = \left(\sum_{k=1}^{n_i}\left|\boldsymbol{r}_{ik}^{(j)}\right|^2 + \sum_{k=1}^{n_j}\left|\boldsymbol{r}_{jk}^{(i)}\right|^2\right)\boldsymbol{I}_d. \quad \ldots\ldots\ldots \quad (6)$$

When the sum of spatial ranks from the i-th group is expressed as

$$\boldsymbol{w}_i^{(j)} = \sum_{k=1}^{n_i}\boldsymbol{r}_{ik}^{(j)} \in \mathbf{R}^{d\times 1}, \quad \ldots\ldots\ldots \quad (7)$$

the expectation of $\boldsymbol{w}_i^{(j)}$ is

$$\mathrm{E}\left(\boldsymbol{w}_i^{(j)}\right) = \mathbf{0} \in \mathbf{R}^{d\times 1}, \quad \ldots\ldots\ldots \quad (8)$$

and the variance of $\boldsymbol{w}_i^{(j)}$ is

$$\mathrm{V}\left(\boldsymbol{w}_i^{(j)}\right) = \frac{n_i n_j}{(n_i+n_j)(n_i+n_j-1)} \cdot \left(\sum_{k=1}^{n_i}\boldsymbol{r}_{ik}^{(j)}\boldsymbol{r}_{ik}^{(j)\mathrm{T}} + \sum_{k=1}^{n_j}\boldsymbol{r}_{jk}^{(i)}\boldsymbol{r}_{jk}^{(i)\mathrm{T}}\right) \in \mathbf{R}^{d\times d}. \quad (9)$$

The multivariate Steel-Dwass test statistic is thus given by

$${W_{ij}}^2 = \frac{2(n_i+n_j)(n_i+n_j-1)d\left|\boldsymbol{w}_i^{(j)}\right|^2}{n_i n_j\left(\sum_{k=1}^{n_i}\left|\boldsymbol{r}_{ik}^{(j)}\right|^2 + \sum_{k=1}^{n_j}\left|\boldsymbol{r}_{jk}^{(i)}\right|^2\right)}. \quad \ldots \quad (10)$$

If ${W_{ij}}^2 \geq q^2(d,c,\infty;\alpha)$, where $q(d,c,\nu;\alpha)$ is the upper α point of the distribution of the d-variate studentized range

with parameters c and ν, the difference between the i-th and j-th groups is significant at level α.[14]

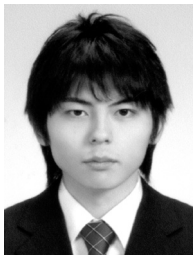

Name:
Takamasa Hattori

Affiliation:
Graduate School of Engineering, Nagoya University

Address:
Furo-cho, Chikusa-ku, Nagoya 464-8603, Japan

Name:
Yoji Yamada

Affiliation:
Professor, Graduate School of Engineering, Nagoya University

Address:
Furo-cho, Chikusa-ku, Nagoya 464-8603, Japan

Brief Biographical History:
1993- Associate Professor, Graduate School of Engineering, Toyota Technological Institute
2004- Group Leader, National Institute of Advanced Industrial Science and Technology (AIST)
2008- Professor, Graduate School of Engineering, Nagoya University

Main Works:
• "Next-generation technology development for mobile and motor function of the human," NTS Inc. 2013

Membership in Academic Societies:
• The Institute of Electrical and Electronics Engineers (IEEE) Robotics and Automation Society
• The Japan Society of Mechanical Engineers (JSME)
• The Robotics Society of Japan (RSJ)

Name:
Shogo Okamoto

Affiliation:
Graduate School of Engineering, Nagoya University

Address:
Furo-cho, Chikusa-ku, Nagoya 464-8603, Japan

Brief Biographical History:
2005 Received B.S. degree in Engineering from Kobe University
2007 Received M.S. degree in Information Sciences from Tohoku University
2010 Received Ph.D. in Information Sciences from Tohoku University
2010- Assistant Professor, Graduate School of Engineering, Nagoya University

Main Works:
• S. Okamoto, "VR-MDS: Multidimensional scaling for classification tasks of virtual and real stimuli," Attention, Perception, & Psychophysics, Vol.76, Issue 3, pp. 877-893, 2014.
• S. Okamoto, H. Nagano, and Y. Yamada, "Psychophysical dimensions of tactile perception of textures," IEEE Trans. on Haptics, Vol.6, Issue 1, pp. 81-93, 2013.
• S. Okamoto and Y. Yamada, "Lossy data compression of vibrotactile material-like textures," IEEE Trans. on Haptics, Vol.6, Issue 1, pp. 69-80, 2013.

Name:
Shuji Mori

Affiliation:
Professor, Faculty of Information Science and Electrical Engineering, Kyushu University

Address:
744 Motooka, Nishi-ku, Fukuoka 819-0395, Japan

Brief Biographical History:
1991- Lecturer, Nagasaki University
1995- Associate Professor, Toyama Prefectural University
2001- Associate Professor, Tokyo Metropolitan University
2006- Professor, Kyushu University

Main Works:
• "Expert anticipation from deceptive action," Attention, Perception, & Psychophysics, Vol.75, pp. 751-770, May 2014.

Membership in Academic Societies:
• The Psychonomic Society
• The Japanese Psychological Association
• The Acoustical Society of Japan

Name:
Shunsuke Yamada

Affiliation:
Mitsui Chemicals, Inc.

Address:
1-5-2 Higashi-Shimbashi, Minato-ku, Tokyo 105-7117, Japan

14. Values of $q(d,c,\infty;\alpha)$ for $d = 2,3,\ldots,6$, $c = 2,3,\ldots,12$, and $\alpha = 0.01, 0.05$ are given in [26].